International Journal of Geospatial and Environmental Research

Volume 1 | Number 2 Article 1

August 2014

Assessing the Impacts of Climate Change, Urbanization, and Filter Strips on Water Quality Using SWAT

Mike Psaris
Portland State University, mike.psaris@gmail.com

Heejun Chang
Portland State University, changh@pdx.edu

Assessing the Impacts of Climate Change, Urbanization, and Filter Strips on Water Quality Using SWAT

Abstract
Precipitation changes and urban growth are two factors altering the state of water quality. Changes in precipitation will alter the amount and timing of flows, and the corresponding sediment and nutrient dynamics. Meanwhile, densification associated with urban growth will create more impervious surfaces which will alter sediment and nutrient loadings. Land and water managers rely on models to develop possible future scenarios and devise management responses to these projected changes. We use the Soil and Water Assessment Tool (SWAT) to assess potential changes in stream flow, sediment, and nutrient loads in two urbanizing watersheds in Northwest Oregon, USA. We evaluate the spatial patterns climate change and urban growth will have on water, sediment and nutrient yields. We identify critical source areas (CSAs) for each basin and investigate how implementation of vegetative filter strips (VFS) could ameliorate the effects of these changes. Our findings suggest that: 1) Water yield is tightly coupled to precipitation. 2) Large increases in wintertime precipitation provide enough sub-surface storage to increase summertime water yields despite a moderate decrease in summer precipitation. 3) Expansion of urban areas increases surface runoff and has mixed effects on sediment and nutrients. 4) Implementation of VFS reduces pollutant loads helping overall watershed health. This research demonstrates the usefulness of SWAT in facilitating informed land and water management decisions.

Keywords
Climate Change, Urban Development, Filter Strips, Stream Flow, Water Quality, SWAT

Acknowledgements
This research was supported by the U.S. National Science Foundation, grant #1226629, and by the Institute for Sustainable Solutions at Portland State University. We would like to thank Rajeev Kapur at Clean Water Services for providing GIS data for our study area. We also appreciate Eugene Foster whose comments help improved the clarity of the manuscript. Thanks also go to the members of the stakeholder workshop for their invaluable input and for their helpful comments. The views expressed are our own and do not necessarily reflect those of sponsoring agencies.

1. INTRODUCTION

Precipitation changes and urban growth are two major factors altering watershed health worldwide (Vorosmarty et al. 2000; Whitehead et al. 2009). The effects of these changes occur at various spatial and temporal scales. Precipitation drives the amount and timing of river flows (Chang et al. 2001; Choi 2008; Franzyk & Chang 2009; Praskievicz and Chang 2011; Tu 2009), and therefore affects sediment and nutrient loads (Atasoy et al. 2006; Chang 2004; Randall and Mulla 2001; Tang et al. 2005; Tong and Chen 2002). Urban growth is the second largest contributor to stream impairments (Paul and Meyer 2001). It increases impervious surfaces causing flashier storm responses, and overland flows carry nutrients more rapidly to streams while reducing the stream's ability to remove them (Meyer et al. 2005; Paul and Meyer 2001; Walsch et al. 2005).

Given these realities, land and water managers are interested in possible solutions to ameliorate the negative changes to water quality. One such possibility is the addition of vegetative filter strips (VFS). These are lands set aside to intercept runoff from crop lands, range lands or other land uses before it enters streams. These areas consist of natural vegetation that removes sediment and nutrients from overland flows (Abu-Zreig 2001; Abu-Zreig et al. 2004). While this does not directly address urban pollutants, this could serve to improve upstream water quality, helping overall watershed health.

The Soil and Water Assessment Tool (SWAT) is a semi-distributed watershed model developed by the USDA's Agricultural Research Service to address the issue of non-point source pollution (Arnold et al. 2011). It has the capacity to model large areas with diverse land uses, and includes algorithms to test the effects of best management techniques, including vegetative filter strips. Niraula et al (2013) used SWAT to identify critical source areas of pollutants in their study basin. Gu and Sahu (2009) used SWAT to locate high impact sub-basins and measure nutrient reductions after installing filterstrips. Lam et al. (2011) assess both the water quality as well as economic impacts of installing filter strips. In this study we investigate the following research questions:

(1) How do water, sediment and nutrient yields change annually and seasonally under precipitation changes and urban growth scenarios?
(2) What are the locations of critical source areas (CSAs) and will these CSAs shift in the future under the combined scenarios of climate change and urban development?
(3) What effect does implementation of VFS have on sediment and nutrient yields?

2. STUDY SITE

2.1 TUALATIN

The 1,829 km^2 Tualatin River Basin roughly shares the borders of Washington County in Northwestern Oregon (Figure 1). The basin is bordered by the Coast Range to the west, Tualatin Mountains (West Hills) to the north and east, and the Chehalem Mountains to the south. With the exception of its headwaters that originate in the Coast Range, the Tualatin River is a low-gradient, meandering river that travels 130 km east, before emptying into the Willamette River. Elevation in the basin ranges from a high of 1,057 m

to a low of 17 m at the river's mouth, and has a mean elevation of 195 m. Soils in the basin formed from weathering of the Columbia River Basalt Group, and deposition of the Willamette Silts by the Missoula Floods during the late Pleistocene. The region has a modified marine climate, dominated by cool wet winters, and warm dry summers. In upper elevations, annual precipitation ranges from 1,330 to 3,280 mm, and average daily temperatures range from 4 to 27°C in the summer and -16 to 12°C in the winter. In the valley, annual precipitation ranges from 740 to 1,850 mm, and average daily temperatures range from 10 to 31°C in the summer, and -10 to 15°C in the winter (Abazoglou 2013).

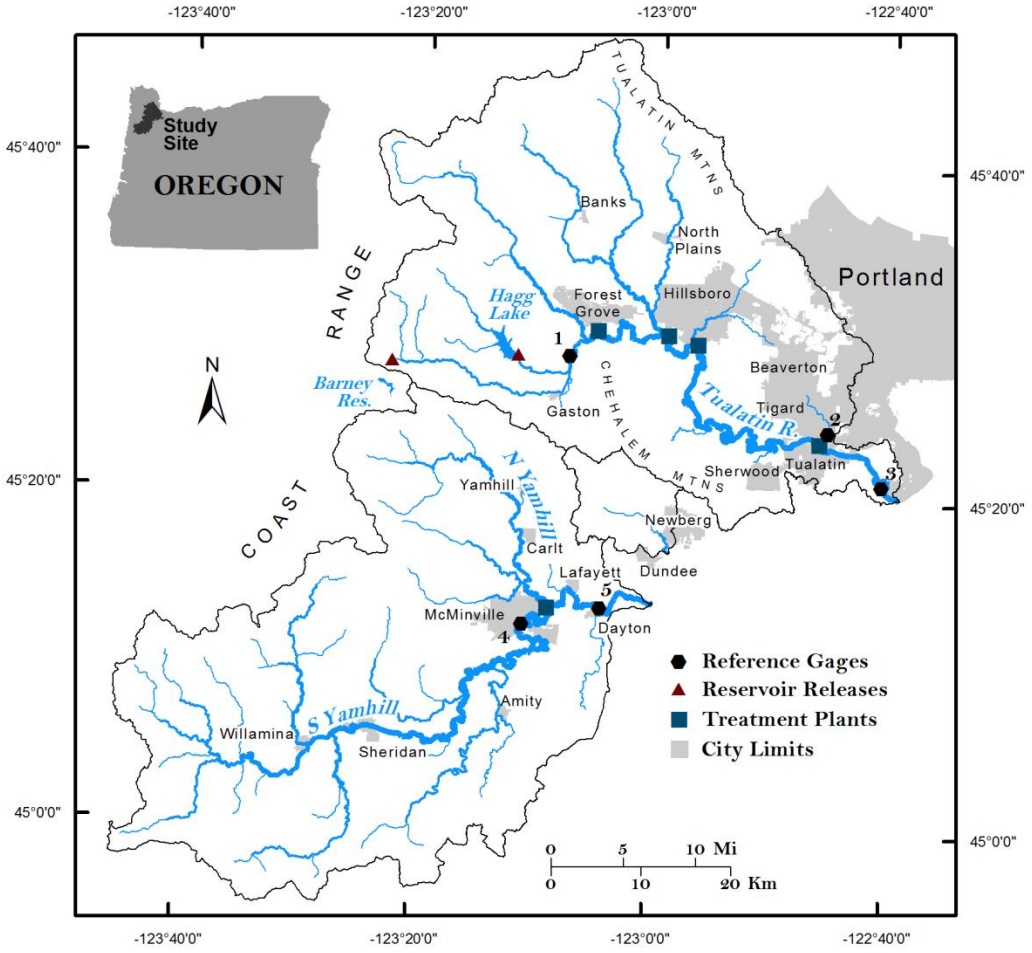

Figure 1. Map of the Tualatin and Yamhill River basins. Gage numbers are referenced in Table 2.

Stream flow is largely rain dominated with peak flows occurring throughout January, and low flows occurring during July. The basin has a runoff ratio of 0.64 based on sixteen

years of flow records (USGS 2012). Two large dams alter the hydrology of the basin. Scoggins Dam on Scoggins Creek provides supplemental flows of around 5.97 cms in the summertime as well as recreational opportunities for local residents. Barney reservoir provides additional flows of around 0.4 cms as an inter-basin water transfer from the Trask River to the upstream portion of the Tualatin. Clean Water Services (CWS) operates four waste-water treatment plants located along the main-stem of the Tualatin River. The two downstream plants, Durham and Rock Creek, process the majority of effluent, while the two upstream plants, Hillsboro and Forest Grove, maintain reserve capacity for anticipated population growth.

Agricultural land dominates the basin. Approximately 49 percent of land in the basin is cultivated, while forested lands comprise 23 percent, and fourteen percent has been developed. The majority of the basin (93 percent) is privately owned. Of public lands, five percent is owned by the State of Oregon and two percent is owned by the Bureau of Land Management (ODEQ 2001).

Due to agriculture, timber harvesting, and rapid urbanization in the mid-twentieth century, the basin suffered from severe algal blooms due to excessive nutrient loadings. In 1988, EPA approved the first set of regulations, known as total maximum daily loads (TMDLs) for dissolved oxygen and ammonia and in 1994 for algae, pH, and phosphorus. In 1998 TMDLs were also approved for temperature (ODEQ 2001). To help improve water quality in the basin, CWS, a designated management agency responsible for improving water quality, has restored riparian zones along tributaries. Riparin restoration incentive programs can reduce thermal loading substantially over time (Cochran and Logue 2011). Additionally, some sections of forest and agricultural lands have implemented best management practices to reduce non-point source pollution in the basin (USEPA 2008). Changes have been made to the TMDLs over the years as needs have arisen, and water quality has improved somewhat (Singh and Chang 2014). However, some rapidly urbanizing areas of the basin still experience water quality problems (Boeder and Chang 2008; Pratt and Chang 2012). Climate change studies in the region indicate that rising air temperatures will accentuate the seasonal range of stream flows, with flows expected to increase in the winter and decrease in the summer (Chang and Jung 2010; Franczyk and Chang 2009; Hamlet and Lettenmaier 1999) and increase stream temperature (Chang and Lawler 2011) and nutrient and sediment exports (Praskievicz and Chang 2011).

2.2 YAMHILL

The Yamhill sub-basin lies to the south of the Tualatin, and drains 1,998 km^2 (Figure 1). The two main rivers, North and South Yamhill, flow southeast and northeast, respectively, until they converge and flow east before emptying into the Willamette River. Elevation in the basin ranges from 1,084 m in the Coast Range to 18 m at the mouth of the Yamhill and has a mean elevation of 217 m. Soils in the basin have similar provenance to those in the Tualatin. Annual precipitation ranges from 1,560 to 3,880 mm in high elevations and 560 to 1,710 mm in lower elevations. Average daily temperatures at high elevations range from -14 to 12 degrees in the winter and 7 to 27 degrees in the

summer. Low elevation daily temperatures range from -10 to 15 degrees in the winter and 10 to 30 degrees in the summer.

The Yamhill River system is much less managed than the Tualatin. There is no major reservoir in the Yamhill to supplement flows or provide flood control, so during the summer measured flows have dropped to as little as 0.04 cms, while winter wet seasons have seen flows as large as 1,141 cms. The runoff ratio is 0.55. Fourty percent of the basin is forested. One third of the basin consists of cultivated crops, and only seven percent is developed. In 1992, EPA approved TMDLs for algae, pH, and phosphorus.

3. DATA AND METHODS

3.1 DATA

The datasets used for model inputs and calibration can be found in Table 1. In order to develop a more complete time series of sediment, nitrogen and phosphorus loads, we use the LOADEST software (Runkel et al. 2004) to estimate a continuous daily time series. These loads were then aggregated to monthly scales for model calibration.

3.2 SWAT MODEL

SWAT is a physically based, semi-distributed daily time-step model (Arnold et al. 1998). It accounts for both terrestrial and in-stream processes. To model flow, SWAT uses the Soil Conservation Service (SCS) curve number approach (SCS 1972). To model sediment transport across the landscape, SWAT uses the Modified Universal Soil Loss Equation (MUSLE, Williams 1975), an event scale variant of the USLE that uses surface runoff instead of precipitation as a measure of erosive energy. The nitrogen mass balance is budgeted into five pools and two main categories. Mineral N consists of the ammonia and nitrate pools, while organic N consists of the fresh organic N (biomass) and active and stable organic N pools. The Phosphorus mass balance is budgeted into six pools split between mineral and organic P. Mineral P consists of the stable, active, and solution pools, while organic P consists of the stable, active, and fresh (biomass) pools (Neitsch et al. 2011). Channel sediment deposition and re-entrainment are modeled using the Simplified Bangold equation. SWAT models in-stream nutrient processes with algorithms from the QUAL2E model (Brown and Barnwell 1987).

SWAT models watershed processes at three spatial scales. The first is the macro-scale, and is essentially the final model output at the mouth of the river. The second meso-scale of analysis is the sub-basin. Sub-basins include stream reaches and their contributing areas. Users can add additional sub-basins by identifying gages or other important watershed characteristics along a stream reach which would warrant a unique spatial demarcation. Finally, the most fundamental unit of analysis in SWAT is the hydrologic response unit (HRU). Each sub-basin has a unique set of HRUs which consist of pixels with similar soil, slope, and land use characteristics. HRUs are aspatial, which means that pixels do not need to be contiguous in order to be grouped together into one HRU. Each HRU can be conceptualized as a field with constant slope, bordering the

stream reach. SWAT calculates the flow, sediment and nutrient yields from an HRU, adds it to what was delivered from the upstream reach, and then calculates in-stream processes assuming a well mixed water column. This conceptualization enables SWAT to aggregate detailed field level processes and management activities up to the watershed scale (Neitch et al. 2011). For example, filter strips and many other best management practices are modeled at the HRU scale. However, the drawback is that the model is not fully distributed and certain spatial processes such as explicit routing of flows between HRUs are not accounted for.

Table 1. SWAT model input data and their sources used in the current study

Model Inputs	Description	Source
Elevation	NHDPlus National Elevation Dataset (NED)	NHD Plus (2010)
Historic Land Cover	National Land Cover Dataset (NLCD, 2006)	USGS (2011)
Urban Growth	NLCD based urban growth scenarios	Hoyer and Chang (2014a)
Stream Network	NHDPlus National Hydrography	NHD Plus (2006)
Soils	The State Soil Geographic Database	STATSGO (2012)
Historic Climate	Gridded Interpolated 4 Km resolution	Abatzoglou (2013)
Future Climate Scenarios	Three Gridded Interpolated GCM's (1979-2065)	Abatzoglou (2012)
Water Quantity and Quality Data	Stream flow; Sediment, nitrogen and phosphorus concentrations	ODEQ (2012) & USGS (2012)
Reservoir and Point Source Releases	Daily releases from Hagg Lake, Barney Reservoir, and WWTPs	CWS (2011) & City of McMinville (2011)
Henry Hagg Lake Specifications	Henry Hagg Lake physical characteristics	Ferrari (2001) & Sullivan and Rounds (2005)

3.3 CALIBRATION AND VALIDATION

We performed manual calibration of SWAT (SWAT 2012, rev. 613) so that interactions between parameters could be captured and multiple calibration objectives could be considered at once. We performed a sensitivity analysis to help inform our parameter selection. We then adjusted the most sensitive parameters to acquire a good fit. We calibrated flow first since it drives sediment and nutrient loads. Since nutrients often travel to the stream bound to sediment we calibrated sediment second and nitrogen and phosphorous last. We used one gage to calibrate the Tualatin, and two additional gages to assess spatial accuracy of Tualatin's calibrated model. We used the USGS Dilley gage (Gage #1 in Figure 1 and Table 2) for calibration since it is unaffected by the four downstream treatment plants. We used two gages to calibrate the Yamhill model. We use the USGS gage in McMinville (Gage # 4 in Figure 1 and Table 2) to calibrate flow, and a station maintained by the Oregon Department of Environmental Quality (Gage # 5 in Figure 1 and Table 2) to calibrate sediment and nutrients.

Table 2. Gages used for model evaluation. F = Flow, TSS = Total Suspended Solids, TN = Total Nitrogen, TP = Total Phosphorus. Gages 1, 4, and 5 were used for calibration.

Gage #	Name	Organization	ID #	Constituents
1	Tualatin River at Dilley	USGS/CWS	14203500	F, TSS, TN, TP
2	Fanno Creek at Durham	USGS/CWS	14206950	F, TSS, TN, TP
3	Tualatin River at West Linn	USGS/CWS	14207500	F, TSS, TN, TP
4	South Yamhill River at McMinnville	USGS	14194150	F
5	Yamhill Water Quality Station	DEQ	10363	S, TN, TP

We measured the efficacy of the model with three metrics suggested by Moriasi (2007): Nashe-Sutcliffe Efficiency (NSE), percent bias (PBIAS), and the RMSE-observations standard deviation (RSR).

The NSE is calculated as

$$NSE = 1 - \frac{\sum_{i=1}^{n}\left(Y_i^{obs} - Y_i^{sim}\right)^2}{\sum_{i=1}^{n}\left(Y_i^{obs} - Y^{mean}\right)^2} \quad (1)$$

where n represents the number of observations, Y_i^{obs} is the i^{th} observed data point, Y_i^{sim} is the i^{th} simulated data point, and Y^{mean} is the mean of all the observed data points. If the model perfectly fits the observed data, NSE equals one. If the model is just as good as taking the mean of the observed data, NSE equals zero. If the mean of the observed data is superior to the model, NSE is less than zero. We aimed to achieve an NSE score of at least 0.5 (Moriasi 2007).

PBIAS is a measure of the model's tendency to either over or under-predict, and is calculated as

$$PBIAS = \frac{\sum_{i=1}^{n}\left(Y_i^{sim} - Y_i^{obs}\right) * 100}{\sum_{i=1}^{n}\left(Y_i^{obs}\right)} \quad (2)$$

If the model on average over predicts, PBIAS is greater than 0. Under-predictions result in a negative PBIAS. According to Moriasi (2007) PBIAS should be less than 25 percent for flow, less than 55 percent for sediment, and less than 70 percent for nutrients. Using the parameters we chose based off of our sensitivity analysis and the recommended goals outlined by Moriasi (2007), reproducing this calibration should be possible. To acquire exactly the same results it would most likely be better to use a deterministic automatic calibration routine. However, given the computational requirements of automatic calibration, and the fact that we did not have a calibration program available which could use the three objective criteria we chose, we felt the best method to consider all three metrics simultaneously was manual calibration.

The third metric is designed to give a description of the model's absolute error, and is calculated as

$$RSR = \frac{RMSE}{STDEV_{obs}} = \frac{\sqrt{\sum_{i=1}^{n}(Y_i^{obs} - Y_i^{sim})^2}}{\sqrt{\sum_{i=1}^{n}(Y_i^{obs} - Y^{mean})^2}} \quad (3)$$

Where $RMSE$ is the root mean square error, and $STDEV_{obs}$ is the standard deviation of the observed data. It is suggested that $RSR \leq 0.7$ for all constituents.

3.5 SCENARIO ANALYSIS

Three downscaled global climate models with future scenarios for the time period 1981-2065 were selected in order to cover a range of possible realities. The GFDL-ESM2M ("low") scenario (MACA 2013) has a 0.08 °C change in average annual temperature, and a 4.47 percent increase in average annual precipitation. The MIROC5 ("medium") scenario (MACA 2013) has a 0.87 °C increase in average annual temperature and a 12.75 percent increase in average annual precipitation. The HadGEM2-ES ("high") scenario (MACA 2013) has a 1.38 °C increase in annual average temperature and a 0.44 percent decrease in average annual precipitation. Seasonal changes for the scenarios can be seen in Figure 2. The low scenario sees precipitation increase in both winter and summer seasons. Precipitation increases during the winter and decreases substantially during the summer in the medium scenario. Finally, precipitation remains roughly the same during the winter, but decreases substantially during the summer in the high scenario.

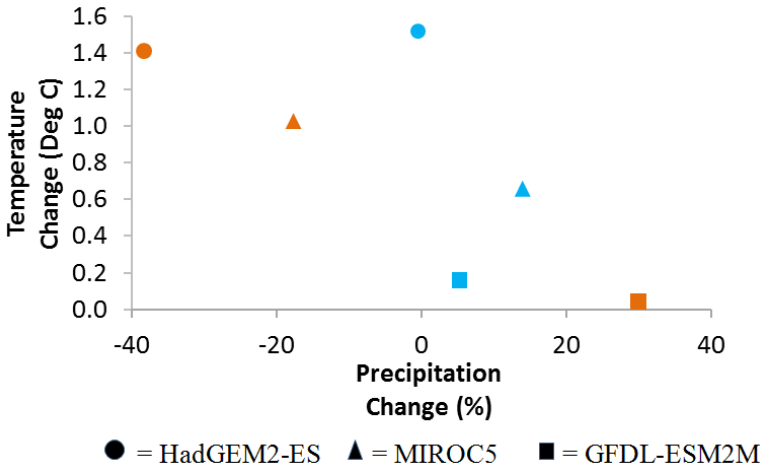

Figure 2. Area weighted changes in precipitation and temperature for each of the three climate scenarios split by season (Winter=DJF, Summer=JJA).

Hoyer and Chang (2014a), with relevant stakeholder consultation, developed land cover change scenarios reflecting possible expansion of urban areas centered on the year 2050. The relative growth of urban areas was based on historical growth rates and projected increases in annual population in the study area. The low scenario assumes an annual growth rate of 0.6 percent and the high scenario assumes a two percent annual

growth rate. Land conversion is based on a graded weight matrix comprised of six factors: urban growth boundary (UGB), distance from the UGB, zoning, groundwater restriction zones, high value farm soils, and measure 49 claims claims which provide exemptions to landowners who purchased land inside the urban growth boundary (UGB) before the UGB regulations were instituted. A spatial mask was used to exclude urban growth from protected lands.

We apply the Vegetative Filter Strip model in SWAT for two representative years in the study period (WY 1994 and 1995). The model was developed from the Vegetative Filter Strip MODel (Munoz-Capena 1999), and designed to apply to HRUs in SWAT. The algorithm permits a percentage of overland flow to be filtered before it leaves an HRU and enters the stream reach. When overland flow encounters vegetation it slows and its sediment carrying capacity becomes reduced. It also provides extra time for runoff to infiltrate the soil and deposit sediment along with it.

For the sake of simplicity, the VFS model in SWAT assumes that the amount of TN and TP filtered out of overland flow is related to sediment reduction. This is assumption is backed up by studies demonstrating that the bulk of nitrogen and phosphorus travel in particulate form off of agricultural fields (White and Arnold 2009).

We apply the vfs model to five sub-basins that exhibit the top five percent sediment and nutrient loads based on a weighted index over the thirty year historic period. The weighted index is comprised of sediment, TN, and TP yields using the following formula:

$$I = 0.5S + 0.25N + 0.25P \tag{4}$$

where, I is the index value, S is the sediment yield (tons/ha), N is the TN yield (kg/ha), and P is the TP yield (kg/ha). We gave sediment the highest weight since in high concentrations it is considered a pollutant and it transports both nitrogen and phosphorus, two nutrients commonly found to exceed natural concentrations as a result of agricultural activities and urban development (ODEQ 2001).

4. RESULTS

4.1 MODEL CALIBRATION

Table 3 reports a summary of the twelve fitted parameter values. Due to a lack of data on sediment erosion across the landscape, and sediment sources and sinks in-stream, we calibrated sediment using MUSLE parameters only. Uncertainties in measured data, LOADEST estimates, and temporal non-stationarity in flow, sediment and nutrient loadings, mean that these values represent estimates of true parameter values only. Metrics were all in acceptable ranges according to Moriasi et al. (2007) during calibration. RSR values for TN and TP at the DEQ gage were slightly higher than the recommended value of 0.7 during validation, but all other metrics were in acceptable ranges. Table 4 shows a summary of monthly model fit metrics. Figure 3 shows calibrated results for flow and sediment for both basins.

Table 3. List of final calibrated parameters for Tualatin and Yamhill sub-basins

Description	Parameter	Min	Max	Tualatin Value	Yamhill Value
Flow					
Baseflow alpha factor (days)	v__ALPHA_BF.gw*	0	1	1	1
Soil evaporation compensation factor	v__ESCO.bsn	0.01	1	1	0
Plant uptake compensation factor	v__EPCO.bsn	0	1	0.01	1
Available water capacity of the soil layer	r__SOL_AWC().sol	-0.2	0.2	-0.2	-0.2
Treshold depth of water in the shallow aquifer required for return flow to occur (mm)	v__GWQMN.gw	0	5000	0.1	0.1
Sediment					
Average slope length	r__SLSUBBSN.hru	10	150	-0.7	-0.4
Min value of USLE C factor applicable to the land cover/plant (Forest)	r__USLE_C.crop.dat	0.001	0.5	0 .01	0.01
USLE equation soil erodibility (K) factor	r__USLE_K().sol	0	0.65	-0.7	-0.3
Average Slope Steepness	r__HRU_SLP.hru	0	1	-0.6	-0.2
Nitrogen					
Nitrogen percolation coefficient	v__NPERCO.bsn	0.1	1	0.01	0.1
Denitrification exponential rate coefficient	v__CDN.bsn	0.1	3	0.1	0.1
Denitrification threshold water content	v__SDNCO.bsn	0.1	1	1	1

*v: Parameter is assigned this value. r: Parameter is multiplied by 1 + this value.

Table 4. Monthly calibration and validation results of flow, sediment, TN, and TP.

	Calibration			Validation		
	NSE	**%BIAS**	**RSR**	**NSE**	**%BIAS**	**RSR**
Dilley*						
Flow	0.93	-0.7	0.27	0.92	-7.8	0.28
Sediment	0.67	53	0.57	0.66	45.7	0.58
TN	0.56	-6.3	0.66	0.76	32.6	0.49
TP	0.65	-26.6	0.59	0.76	-1.1	0.49
Yamhill*						
Flow	0.92	-16.4	0.28	0.91	-16.6	0.30
Sediment	0.69	-9.4	0.55	0.82	11.8	0.42
TN	0.51	24.4	0.7	0.57	20.7	0.73
TP	0.54	1.2	0.68	0.72	25.8	0.72
Fanno						
Flow	0.92	0.9	0.28	0.9	1.7	0.31
Sediment	0.17	-57.4	0.91	0.08	-61.6	0.96
TN	0.24	-34	0.87	0.14	-30.9	0.93
TP	0.32	-55	0.82	0.32	-53.7	0.82
West Linn						
Flow	0.93	11	0.27	0.94	9.5	0.25
Sediment	0.63	52.2	0.61	0.29	118.6	0.84
TN	0.6	-33	0.63	0.67	3.6	0.57
TP	0.28	-57.5	0.85	0.57	-40.4	0.66

*Gages used for calibration and validation

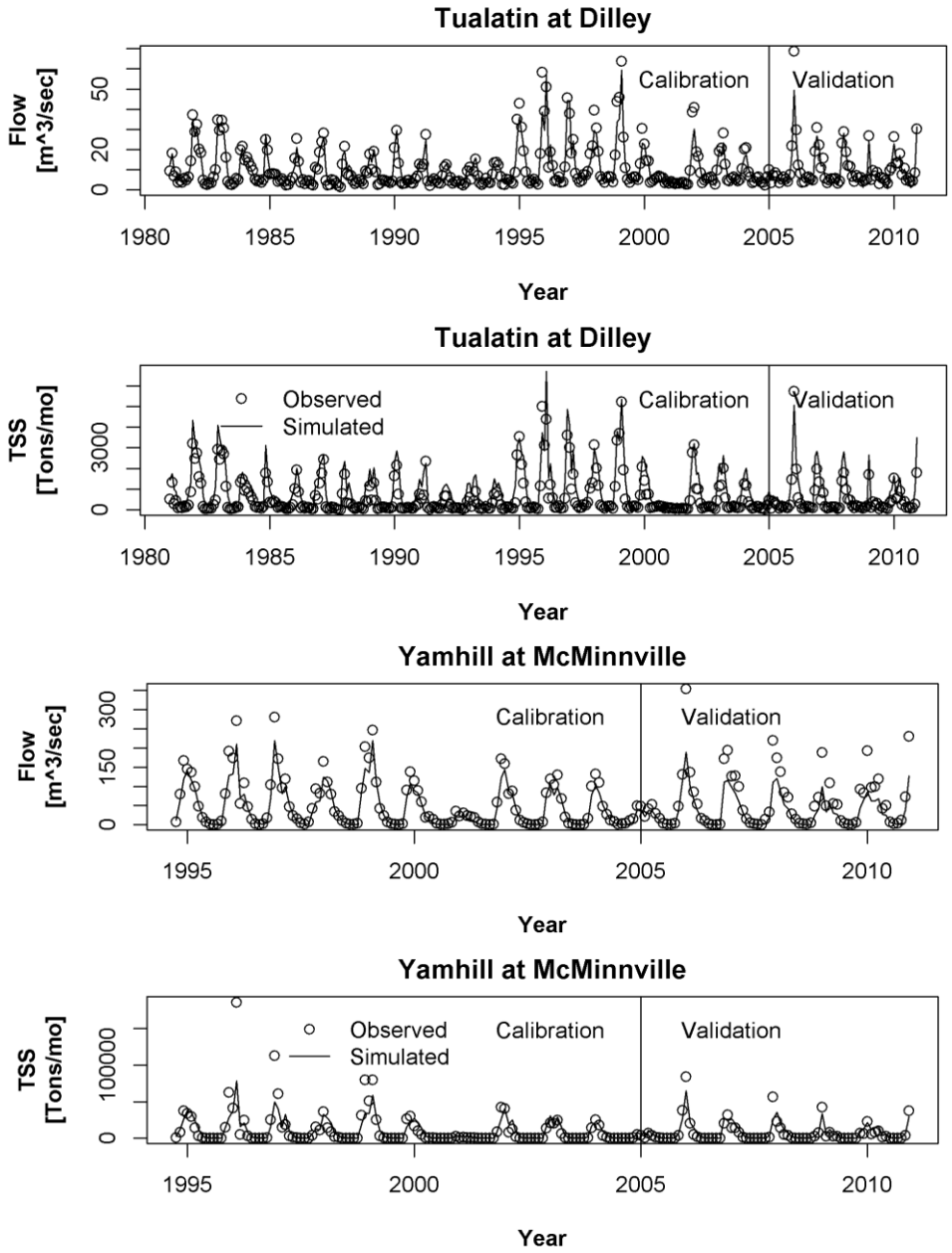

Figure 3. Comparison of monthly simulated and observed flows and sediment loads for Tualatin and Yamhil.

4.2 Future Changes under Climate and Land Cover Change Scenarios

Average annual basin-wide flows increase in all scenarios due to the combination of urbanization and increased precipitation. While there is a slight decrease in annual

precipitation in the high climate scenario, impervious surfaces decrease infiltration and contribute to a slight increase in annual water yield (Table 5).

Table 5. Percent change in annual and seasonal precipitation and flow for Tualatin and Yamhill under climate change and urban growth scenarios.

	Tualatin			**Yamhill**		
	Precipitation	**Flow**		**Precipitation**	**Flow**	
Climate		**Land Use**			**Land Use**	
		Low	**High**		**Low**	**High**
	Annual					
Low	5.17	6.1	6.14	4.15	6.2	6.29
Medium	12.72	18.8	19.13	13.13	24.61	19.47
High	-0.12	0.86	1.12	-0.25	0.69	0.04
	Winter					
Low	6.3	6.07	6.07	4.3	7.33	7.34
Medium	13.36	16.23	16.22	14.04	16.81	16.79
High	-0.35	6.41	6.4	-0.14	4.86	4.87
	Summer					
Low	31.85	25.16	25.16	30.05	18.97	19
Medium	-16.49	5.67	5.32	-19.14	8.08	8.03
High	-40.24	-30.16	-30.9	-36.56	-28.11	-28.14

Changes in wintertime flows follow the same pattern as annual flows since a significant portion of precipitation falls during winter months. In all scenarios wintertime flow increases by a greater percentage than precipitation due to increased impervious surfaces. Fall is the only season where precipitation increases in the high climate scenario (Figure 4). The slight lag between precipitation and runoff means that flows still increase during the winter despite a slight decrease in rain in winter. The lag between runoff and precipitation can be seen clearly in all scenarios. Peak flows typically occur a month or two after precipitation (Figure 4).

Summertime flows have a mixed response. In the low climate scenario flows increase by a smaller percentage than precipitation due to increased evapotransporation. In the medium climate scenario, summer-time flows contain a large baseflow component due to large winter and spring rains. These groundwater inputs enable summer-time flows to increase despite a decrease in summer precipitation greater than 15 percent. Under the high scenario, summer-time flows decrease by a smaller percentage than precipitation due to less evapotranspiration.

(a)

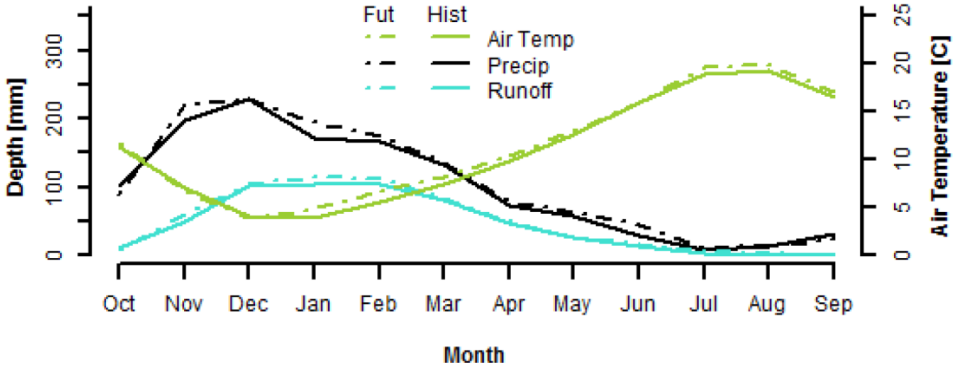
Fut
Hist
Air Temp
Precip
Runoff
Depth [mm]
0
100
200
300
Air Temperature [C]
0
5
10
15
20
25
Oct
Nov
Dec
Jan
Feb
Mar
Apr
May
Jun
Jul
Aug
Sep
Month

(b)

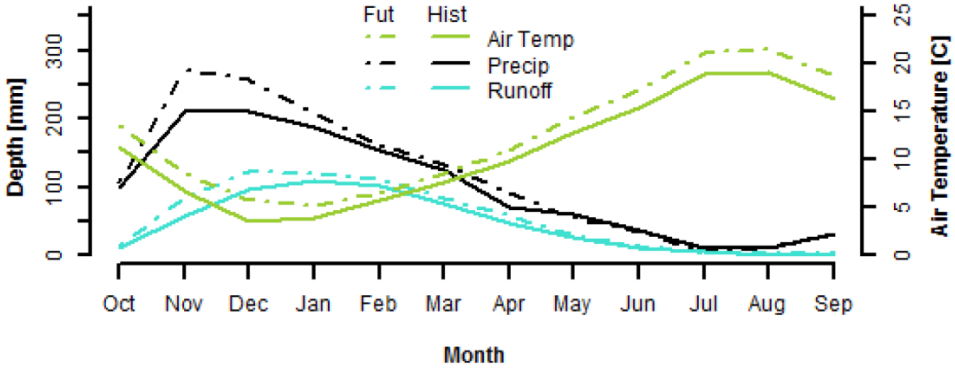
Fut
Hist
Air Temp
Precip
Runoff
Depth [mm]
0
100
200
300
Air Temperature [C]
0
5
10
15
20
25
Oct
Nov
Dec
Jan
Feb
Mar
Apr
May
Jun
Jul
Aug
Sep
Month

(c)

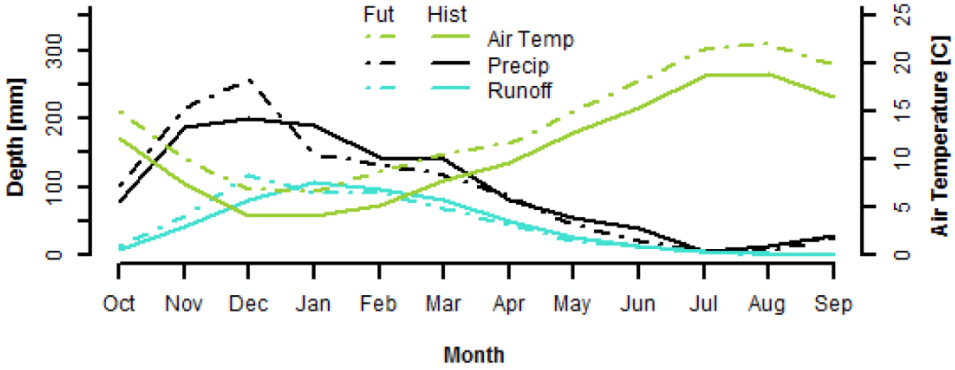
Fut
Hist
Air Temp
Precip
Runoff
Depth [mm]
0
100
200
300
Air Temperature [C]
0
5
10
15
20
25
Oct
Nov
Dec
Jan
Feb
Mar
Apr
May
Jun
Jul
Aug
Sep
Month

(e)

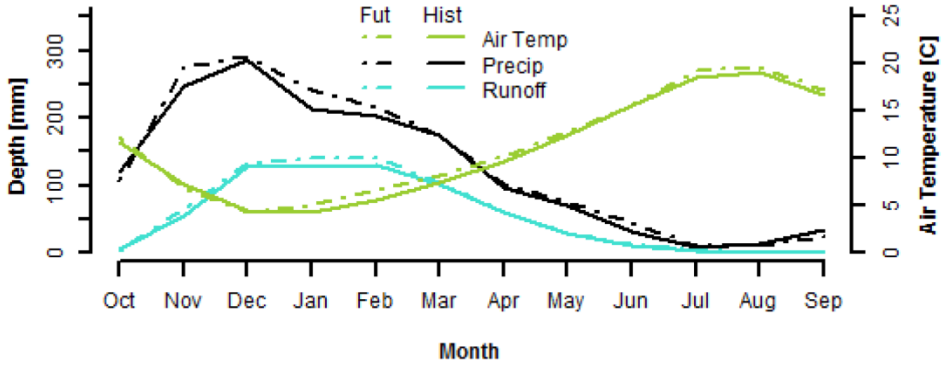

(f)

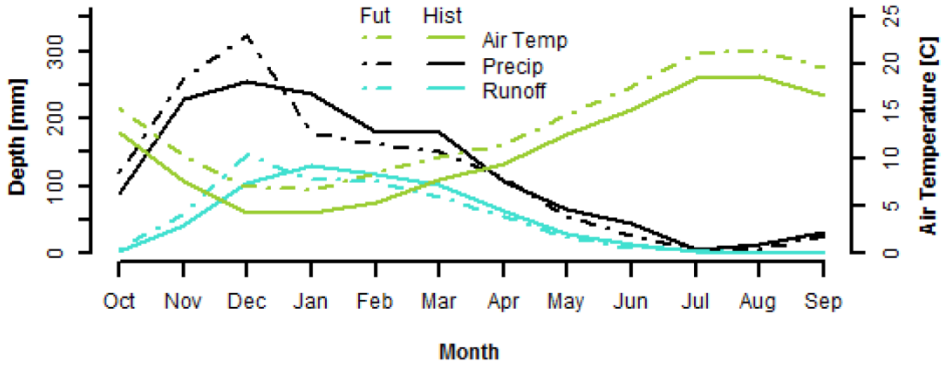

(g)

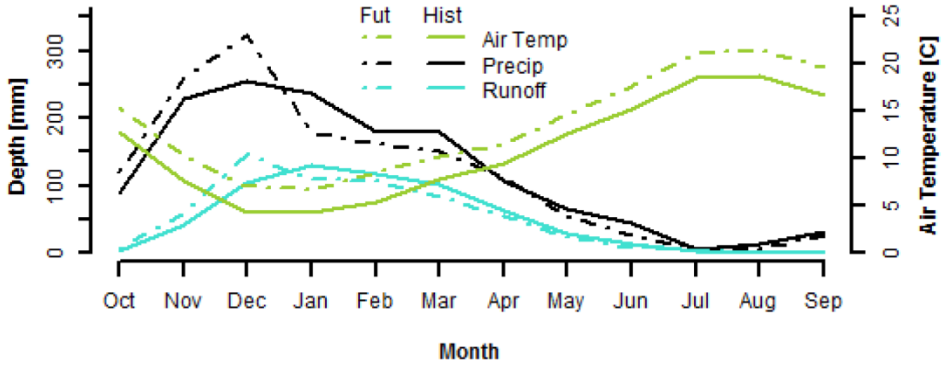

Figure 4. Changes in precipitation, air temperature, and flow for the high urban scenario for Tualatin: low (a), medium (b), and high (c) climate scenarios. Yamhill: low (e), medium (f), high (g) climate scenarios.

At the annual scale the spatial patterns of changes to water yield are fairly uniform and reflect changes in precipitation (Figure 5). A few sub-basins that are located in near urban areas see significant decreases in percolation due to urbanization and therefore have increases in annual water yield as high as 31 percent. These patterns are the same throughout the winter months. During the summer months (Figure 6), urbanized areas have less groundwater to supplement flows. As a result, these sub-basins see decreases in the medium and high scenario, both of which have decreased summer precipitation. The low scenario has more summer precipitation, so the urban areas see summer water yield increase.

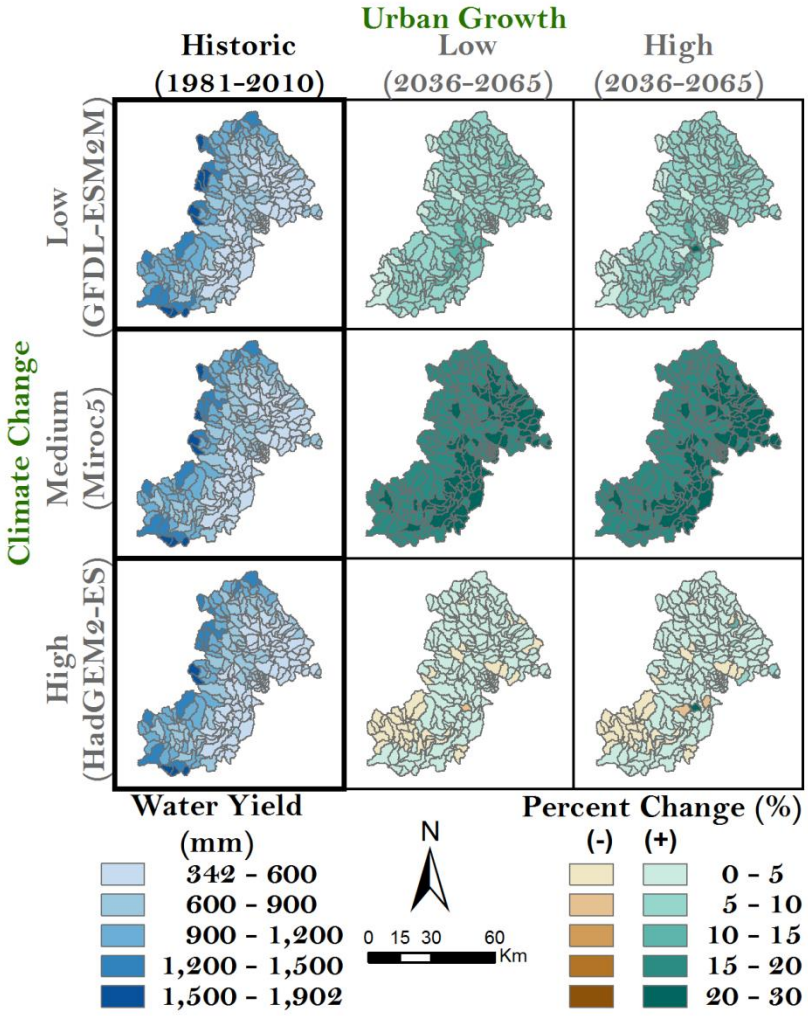

Figure 5. Percent change in average annual water yield by sub-basin under climate change and urban growth.

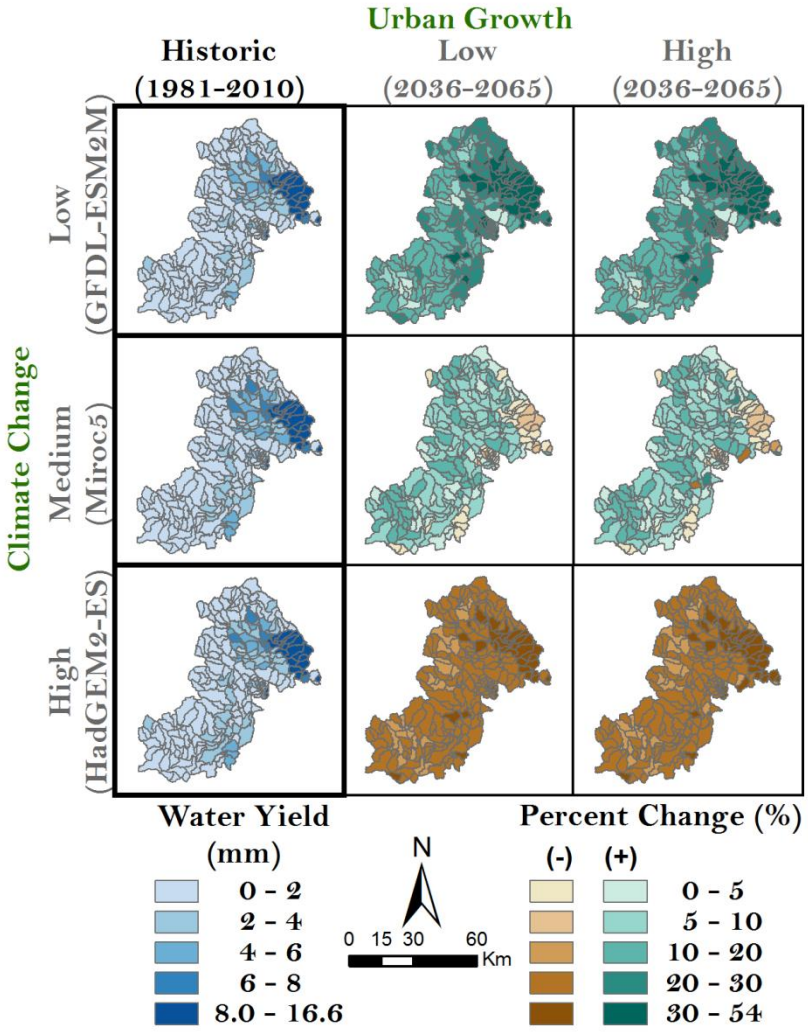

Figure 6. Percent change in average summer water yield under climate change and urban growth.

There are basin-wide decreases in sediment in Tualatin under the low scenario annually and during the winter due to increases in impervious surfaces (Table 6). Erosion increases during the summer due to a 31.8 percent increase in precipitation. Yamhill sees uniform increases in sediment under the low climate scenario due to less urban growth which permits moderate increases in precipitation to increase erosion. Both basins see increases in sediment during the medium scenario, reflecting the universal increase in precipitation and flows for the basin. While Tualatin sees sediments increase under the high climate scenario both annually and during the winter, Yamhill has a decrease

annually and a slight increase during the winter. Some of the shifts in sediment seem counter intuitive when compared to the precipitation changes.

Table 6. Percent change in annual and seasonal sediment loadings under climate change and urban growth

	Tualatin		**Yamhill**	
Climate	**Land Use**			
	Low	**High**	**Low**	**High**
	Annual			
Low	-7.6	-7.64	6.5	6.77
Medium	38.5	48.17	29.6	22.19
High	17.58	27.69	-2.84	-2.63
	Winter			
Low	-11.95	-11.95	6.88	7.26
Medium	33.85	42.29	16.22	16.63
High	24.27	33.9	1.75	2.03
	Summer			
Low	81.96	82	73.06	73.04
Medium	6.82	13.38	5.62	5.42
High	-44.37	-42.45	-38.91	-39

The spatial patterns of sediment yields suggest areas of high slope exhibit the highest sediment yields (near the basin boundaries), reflecting the important role slope plays in erosional processes (Figure 7). Cultivated agricultural lands are located on fairly flat terrain, and therefore do not exhibit erosion rates as high as those for hay and rangeland which are located on a mix of flat and high sloping areas. Changes in erosion resulting from climate change respond in unpredictable ways. Forest, hay and range lands may see increases in erosion under one climate scenario, but see a decrease in another. Neither land cover, nor slope appears to dictate this pattern. Urban areas see a consistent increase in erosion rates.

Total nitrogen travels to the stream through lateral flow, overland flow, and transport with sediment. TN increases annually and during the winter for all climate scenarios reflecting increased transport from higher flows (Table 7). The only decreases are seen under the medium and high climate scenarios where there are decreases in precipitation. Yamhill sees either smaller increases, or larger decreases under the high urbanization scenarios due to conversion of high nutrient yielding lands to lower yielding urban lands. Tualatin sees this same pattern for the medium climate scenario, but more mixed results for the low and high scenarios.

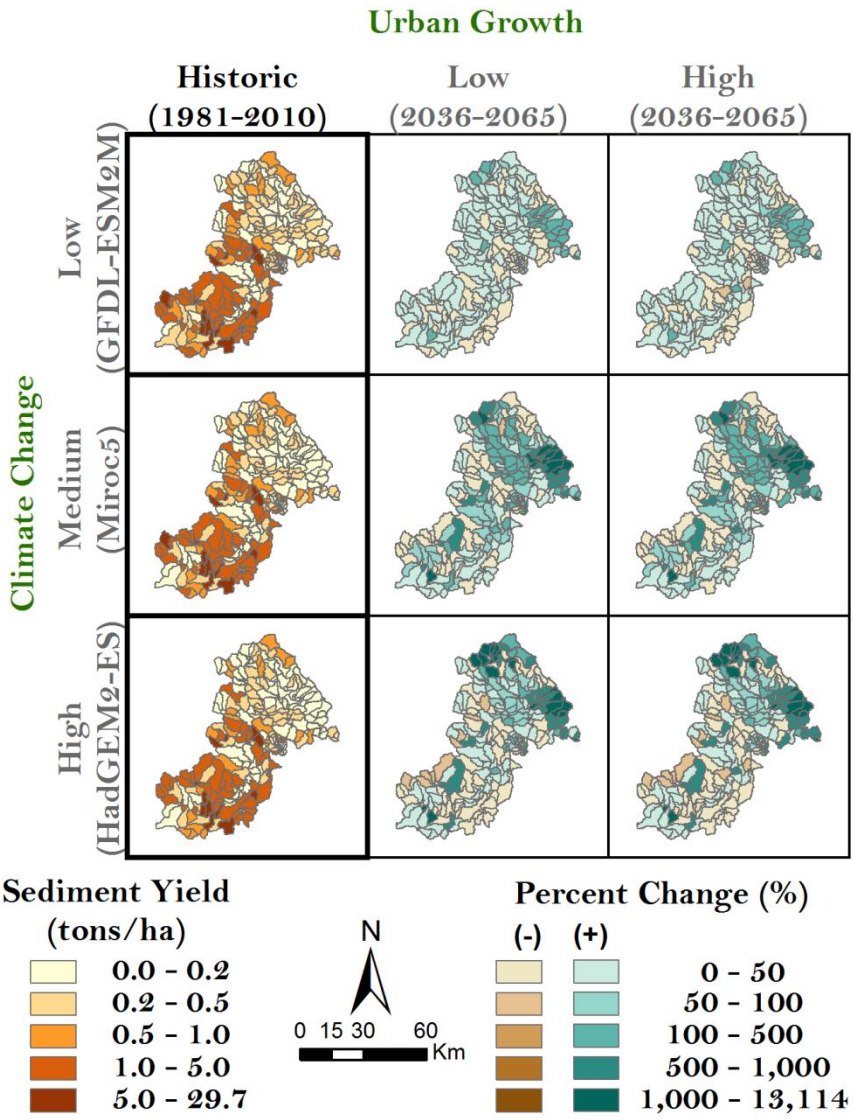

Figure 7. Percent change in annual average sediment yields under climate change and urban growth.

Spatial patterns of TN yield show the importance of slope (Figure 8). Range lands and lands under hay production with higher slopes produce the highest yields. Cultivated agricultural lands lie on more gently sloping valley lands and do not demonstrate as heavy an impact in the model. Urbanizing sub-basins show large increases in nutrients. Areas which have historically low nutrient yields also see greater proportionate increases in yields. These patterns closely follow those of sediment.

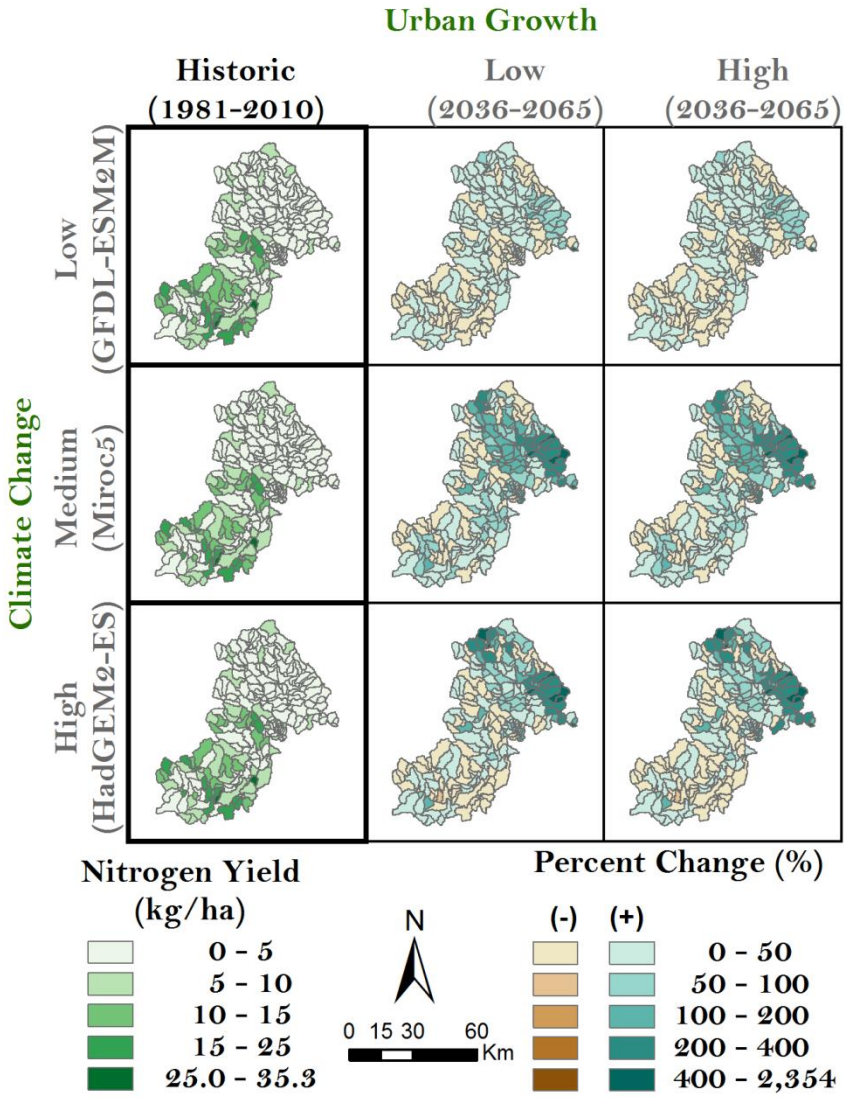

Figure 8. Percent change in annual average TN yield under climate change and urban growth.

Total phosphorus travels to the stream attached to sediment, in solution with overland flow, in mineral form, and with groundwater. The Tualatin sees annual increases in TP throughout all climate scenarios, while Yamhill sees an increase only in the medium scenario (Table 8). In Yamhill, the high urban growth scenarios show slightly larger decreases in annual and winter TP loads than the low urban growth scenario. In the summer Yamhill has slightly larger increases or slightly smaller decreases in the high urban growth scenario. The largest increases in TP occur during the summer in the low climate scenario due to a thirty percent increase in precipitation.

Table 7. Percent change in annual and seasonal TN loadings under climate change and urban growth.

	Tualatin		Yamhill	
Climate	**Land Use**			
	Low	**High**	**Low**	**High**
			Annual	
Low	13.9	13.93	4.6	4.07
Medium	48.7	48.27	21.67	21.01
High	28.15	28.26	2.78	2.20
			Winter	
Low	17.75	17.75	6.25	5.52
Medium	59.38	59.07	20.49	19.62
High	56.83	57.14	12.65	11.78
			Summer	
Low	78.6	78.61	64.6	63.88
Medium	0.002	-1.58	-31.97	-32
High	-64.04	-64.24	-70.55	-70.83

Table 8. Percent change in annual and seasonal TP loadings under climate change and urban growth.

	Tualatin		Yamhill	
Climate	**Land Use**			
	Low	**High**	**Low**	**High**
			Annual	
Low	4.7	4.67	-15.7	-15.83
Medium	68.8	73.94	1.55	1.47
High	58.75	64.93	-17.85	-17.89
			Winter	
Low	1.12	1.12	-18.32	-18.51
Medium	57.11	60.9	-11.51	-11.66
High	78.77	85.13	-17.82	-17.87
			Summer	
Low	359	359	596.21	598.38
Medium	-57.24	-52.4	-76.97	-76.08
High	-77.69	-75.74	-70.8	-70.37

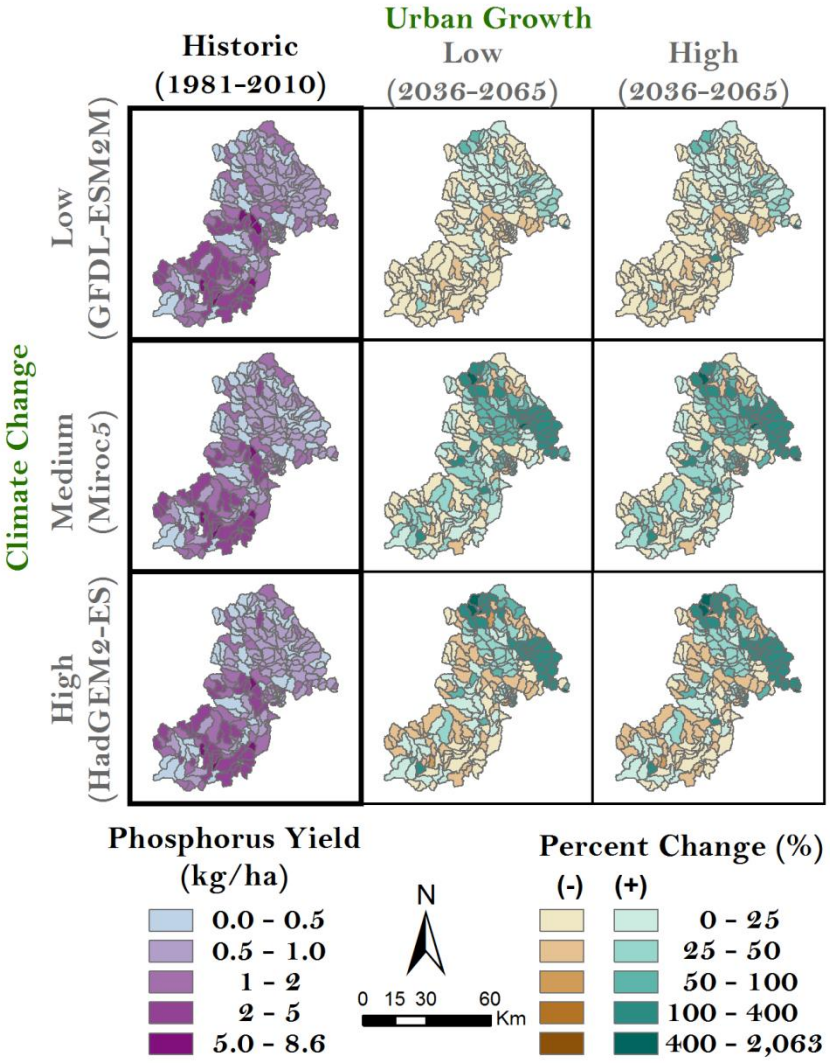

Figure 9. Percent change in annual average TP yields under climate change and urban growth.

Spatial patterns of TP follow those of sediment. There are large increases in the Portland metro area as well as in the higher elevations of the coast range in the Tualatin (Figure 9) as a result of high sloping urban lands and areas harvested for timber.

4.3 Location of CSAs

The top one percent of sub-basins have an average index of 19.4. The bottom one percent have an average index of 0.05. Out of the sub-basins in the study site, the top twelve percent are in the Yamhill basin, signifying the proportionately high sediment exports

predicted by the model. The top five percent index values for each basin can be visualized in Figure 10. Many CSA's remain the same while some hotspots shift according to the spatial patterns created by climate change and urbanization discussed previously. The high climate scenario sees six CSAs shift. The medium scenario sees five shift, and the low scenario sees only three CSAs shift.

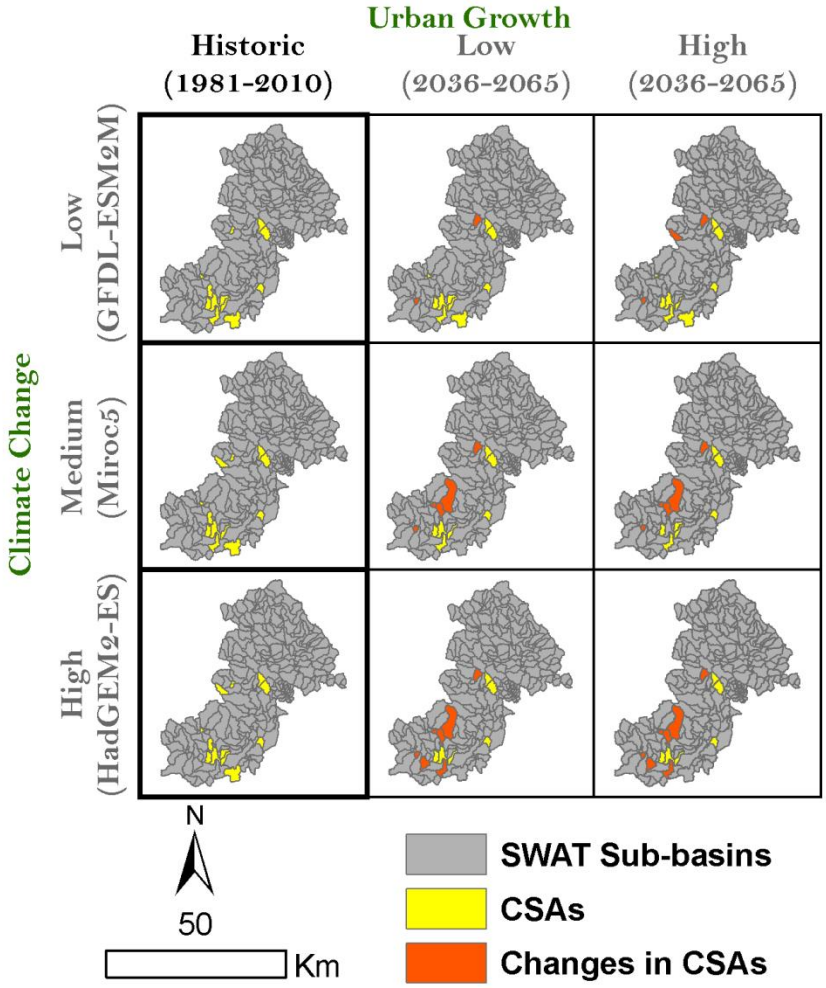

Figure 10. Shifts in hotspots due to climate change and urbanization.

At the HRU level, relationships between land cover and topography can be seen more directly than at the sub-basin scale due to averaging. Hotspots at the HRU scale consist of high sloping hay and range land. The average basin-wide slope in Tualatin is 14.7 percent, while the area weighted average slope for HRU CSAs is 30.5 percent. In Yamhill, the basin-wide slope is 17.3 percent, while the average slope for HRU CSAs is 23.7 percent. The dominant land use in HRU CSAs for Tualatin is rangeland (88%) and

hay (12%). The dominant land use in HRU CSAs for Yamhill is Hay (54%) and rangeland (46%).

4.4 MANAGEMENT

Application of vegetative filter strips has an average rate of reduction of 61.4 percent for erosion, 49.2 percent for TN, and 62.9 percent for TP. The low flow year had a larger reduction in sediment and nutrients (S: 65.7, TN: 51.2, TP: 65.5%) than the high flow year (S: 57.7, TN: 47.3, TP: 60.3%). Index values dropped on average 54.5 percent, bringing all but the most extreme sub-basins out of the top five percent (Table 9).

Table 9. Comparison of top 5% sub-basins before and after VFS applied

No management		VFS	
Index	**Rank**	**Index**	**Rank**
31.07	1	15.66	1
16.55	2	7.50	16
16.51	3	7.13	19
13.79	4	6.54	25
12.81	6	5.24	33

5. DISCUSSION

5.1 MODEL CALIBRATION

Results of model calibrations were mixed (Table 4). Flow simulations closely match observed data in both basins, and the spatial patterns of water yield make sense given the known orographic effects of the coast range (Figure 11).

Sediment calibration in the Yamhill was acceptable. Model assessment at other parts of the Yamhill was not possible due to lack of data, but the homogenous land cover characteristics throughout the basin may make it safe to assume the model performs well throughout. Sediment calibrations in the Tualatin were acceptable at the Dilley and West Linn gage. However, the Fanno gage needs improvement. The poor performance is likely due to SWAT's inability to effectively capture physical processes unique to urban areas. SWAT assumes urban areas consist of impervious surfaces and Bermuda grass. This assumption is likely too simplistic. For example, we'd expect SWAT to under predict sediment loads in urban areas which have yards with more exposed soils. This may be one explanation for the negative bias in sediment results. However, this alone cannot account for SWAT's deficiencies in Fanno Creek since the NSE and RSR are also poor, meaning the model is not simply under predicting, but differs erratically from the observed data. One possible explanation is that SWAT cannot capture in-stream processes unique to small urban watersheds. Urban streams are known to function

differently than undisturbed streams. In particular, a larger percentage of sediment originates from channel erosion rather than hill slope processes (Paul and Meyer 2001). This channel erosion can happen in response to storm events, or as a result of construction near the stream. These types of discontinuous processes would cause sediment loads to vary sporadically over both short and long time periods, and may explain SWAT's poor performance. Spatial patterns of sediment yield are sensible, but due to the poor calibration results for Fanno Creek, the results in this part of the basin have less certainty. As a result, our confidence in the precise changes that may take place is lower in Fanno Creek than in other portions of the basin.

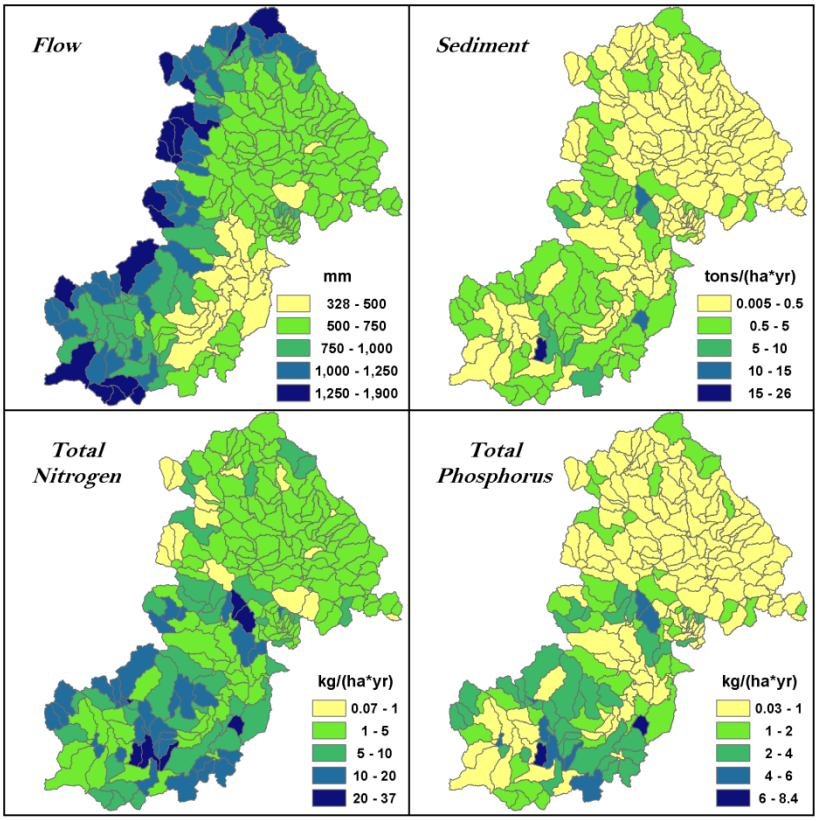

Figure 11. Spatial patterns of flow, sediment, total nitrogen, and total phosphorus.

Nutrient calibrations are acceptable for the Dilley and Yamhill DEQ calibration points, but were unsatisfactory for the West Linn and Fanno gages. This makes sense since there are two waste water treatment plants above the West Linn gage which release water with varying concentrations of nutrients throughout the year. While flow from these plants were included in the model, estimates of nutrient concentrations were difficult to derive. As a result these sources of nutrients were excluded from the model. This would explain the under prediction of both TN and TP at the West Linn gage. As for Fanno Creek, since nutrients tend to travel with sediment, the poor sediment results may

also explain the poor nutrient results. Spatial patterns of nutrient yield appear sensible in the Tualatin where yields roughly track sediment yields.

5.2 SPATIAL PATTERNS OF FLOW, SEDIMENT, AND NUTRIENTS

The spatial patterns of SWAT output can be seen in Figure 11. These patterns constitute a mix of natural processes, model structure, and underlying model assumptions. Orographic effects from the Coast Range create a clear east-west gradient in water yield with higher yields in the higher elevations to the west, and lower yields in the valleys of the two basins. A similar spatial pattern of flow was found in another study for the area using a landscape model InVEST (Integrated Valuation of Environmental Services and Tradeoffs) (Hoyer and Chang 2014b). Summer water yield is larger in urban areas (Figure 6) than the rest of the basin. One would expect baseflow in the higher elevations to sustain water yield throughout the basin at higher levels than the urban areas. A more complete analysis of sub-surface flows in the model could explain why this pattern is taking place. One explanation is that baseflows during the summer are not enough to overtake the immediate runoff that will take place in urban areas.

There are intra- and inter-basin spatial patterns for sediment. Predicted terrestrial yields in the Tualatin are uniformly smaller than those in the Yamhill. This disparity is likely due to in-stream processes in the model not being properly calibrated. This type of calibration could be done in the future using a submerged jet to characterize the erosion taking place when stress is applied to the channel surface (Allen et al. 1999; Hanson 1990). This is resource intensive, and results are likely to vary throughout the stream network based on particle size distribution (Kaufmann et al. 2008). It should be noted that SWAT's default sediment routing algorithm, the simplified Bangold equation assumes all sediment is of silt size, and it does not partition erosion between the stream bank and stream bed. More advanced routines are available that do take into account particle size. However, it is still incumbent on the user to define the median particle diameter.

At the time of this writing, no field studies could be found detailing sediment yields off the landscape. A study using the EPIC model in the Tualatin exists (Moberg 1995), but no empirical data were used. Moberg (1995) recommends further field scale data collection, but no study has yet been completed. As a result of default in-stream sediment processes, higher in-stream sediment yields are apportioned directly to terrestrial erosion in this study.

Intra-basin variation is due to the combination of landscape factors such as land uses and slopes. In the Tualatin, modeling results indicate that the majority of erosion is due to clear-cuts located on high slopes throughout the Coast Range. Since cultivated agricultural lands are found more frequently on low to medium slopes in the Tualatin, there is less opportunity for severe erosion to take place. In the Yamhill, the most severe erosion comes from lands classified as hay which reside on steeper slopes. In both basins forested areas contribute least to erosion due to the soil's thick layers of humus and protection from rain splash erosion. Similar results were reported in another study that compared urban, mixed, and forested watersheds in the Portland metro area (Chen and Chang 2014).

Much of the nutrient loads into streams travel either bound to clay or in solution with overland flow, so sub-basins with higher sediment yields also see higher nitrogen and phosphorus yields. This explains the similar inter-basin patterns for TN and TP. While studies have shown a relatively higher phosphorous concentration in the Tualatin River due to naturally occurring concentrations of phosphorus in the Hillsboro Formation (Wilson et al. 1999), the similar progeny of soils extant in both basins suggest this pattern is present in Yamhill as well (email correspondence with Scott Burns, Ph.D, Geology, Portland State University, Oct. 9th, 2013). Thus, the inter-basin differences in phosphorus are mainly due to its relationship with sediment.

5.3 FUTURE CHANGES AND ADAPTIVE MANAGEMENT

While there are decreases in sediment and nutrients basin-wide under some scenarios, urban areas consistently show increases. This finding is consistent with many previous studies (Franczyk and Chang 2009; Praskievicz and Chang 2011; Tong and Chen 2002; Tu 2009). While the direction of changes in urban areas is consistent, there is a wide range of responses to climate change scenarios. This is due in large part to the inherent uncertainty in climate models (Chang and Jung 2010; Praskievicz and Chang 2009) and the additional uncertainty in the hydrological model response to these climate models. The most potent example of this in our study is the finding that flows increase in the summer despite summertime reductions in precipitation in the medium scenario. The wide variations in hydrological response stress the need for adaptive water resource planning that incorporates these uncertainties into infrastructure design while scientists work to develop climate models with more accuracy and precision.

This study also demonstrates the potential for using SWAT to locate CSAs, and identify changes over time. The methodology employed in this study can be used to help identify possible areas for BMP installation, with vegetative filter strips being just one example. While this research suggests that VFS could be used as a method of promoting sustainable land management practices under the stress of future climate change and ongoing urban development, there are many other tools available such as biofiltration (Hatt et al. 2009; Read et al. 2008), riparian buffers (Wagner 2008), and permeable pavements (Barattebo et al. 2003).

Because the use of SWAT to identify CSAs is new, and few studies have validated CSAs identified by SWAT (Niraula et al. 2013), further research is needed to validate the model's use for this purpose. Collecting detailed land, soils, and water quality information at the local scale is needed before using the CSAs identified in this study to guide regulatory activities.

6. CONCLUSIONS

Changes in precipitation levels and urban growth are two main drivers that threaten watershed health in the future. This study focusses on assessing hydrologic and water quality changes to precipitation and urban growth, and investigates how the application of vegetative filter strips might ameliorate these effects.

Flows typically follow precipitation trends, but some non-linear effects result from seasonal soil water storage permitting summer flows to increase despite reductions in summer rains. Urban areas show larger increases in annual flows due to high percentages of impervious surfaces. Winter flow changes are similar to annual changes, but summer flows are projected to decline.

As flow increases, annual sediment yields increase basin-wide in most scenarios. Urban areas display particular sensitivity to increases in sediment yields, possibly due to their historically small yields relative to other land uses. TN yields increase basin-wide in most scenarios. High sloping regions with hay and rangelands have the highest TN yields. Urban areas show the greatest sensitivity to future climate and land use changes. TP yields increase in exactly half of the scenarios, however the percent increases in these scenarios is greater than the decreases. Spatial patterns of TP yields follow those of sediment. The greatest increases can be seen in urban lands. These findings suggest that urban areas can be targeted for reducing high flows and additional nutrient and sediment loads.

CSA are located in areas of high slopes and hay or range lands. CSA shifts under urban growth and climate change, suggesting that managers could use models to identify areas deserving extra regulatory attention. However validation through field studies is required before model output can be trusted. Changes in CSAs appear to be related more to climate change than urban growth in this study. Implementation of VFS reduced sediment and nutrient loads to the stream, suggesting this should be promoted as a best management practice for land owners.

The results of this study suggest that SWAT is a useful tool for identifying target areas for reducing nutrient and sediment loads and evaluating the effects of alternative land management on nutrient and sediment loads under the pressure of climate change and urban growth. Future studies should focus on validating CSAs identified by SWAT and characterizing downstream effects resulting from best management practices.

REFERENCES

Abatzoglou, J.T. (2013) Development of Gridded Surface Meteorological Data for Ecological Applications and Modeling. *International Journal of Climatology*, 33, 121-131.

Abatzoglou, J.T., and Brown, T.J. (2012) A Comparison Of Statistical Downscaling Methods Suited for Wildfire Applications. *International Journal of Climatology*, 32, 772-780.

Abu-Zreig, M., Rudra, R.P., Whiteley, H.R., Lalonde, M.N. and Kaushik, N.K. (2003) Phosphorus Removal in Vegetated Filter Strips. *Journal of Environmental Quality*, 32, 613-619.

Abu-Zreig, M., Rudra, R.P., Lalonde, M.N., Whiteley, H.R. and Kaushik, N.K. (2004) Experimental Investigation of Runoff reduction and sediment Removal by Vegetated Filter Strips. *Hydrological Processes*, 18, 2029-2037.

Allen, P.M, Arnold, J. and Jakubowski, E. (1999) Prediction of Stream Channel Erosion Potential. *Environmental and Engineering Geoscience*, 5, 339-351.

Arnold, J.G., Srinivasan, R., Muttiah, R.S. and Williams, J.R. (1998) Large Area Hydrologic Modeling and Assessment Part I: Model Development. *Journal of the American Water Resources Association*, 34(1), 73-89.

Arnold, J.G., Moriasi, D.N., Gassman, P.W., Abbaspour, K.C., White, M.J., Srinivasan, R., Santhi, C., Harmel, R.D., van Griensven, A., Van Liew, M.W., Kannan, N. and Jha, M.K. (2012) SWAT: Model Use, Calibration, and Validation. *Transactions of the ASABE*, 55(4), 1491-1508.

Atasoy, M., Palmquist, R.B. and Phaneuf, D.J. (2006) Estimating the Effects of Urban Residential Development on Water Quality Using Microdata. *Journal of Environmental Management*, 79, 399-408.

Brattebo, B.O. and Booth, D.B. (2003) Long-term Stormwater Quantity and Quality Performance of Permeable Pavement Systems. *Water Research*, 37, 4369-4376.

Boeder, M. and H. Chang. (2008). Multi-scale Analysis of Oxygen Demand Trend in an Urbanizing Oregon Watershed. *Journal of Environmental Management*, 400(1-3), 567-581.

Brown, L.C. and Barnwell Jr., T.O. (1987) The Enhanced Water Quality Models QUAL2E and QUAL3E-UNCAS Documentation and User Manual. EPA document EPA/600/3-87/007. USEPA, Athens, GA.

Chang, H., Evans, B.M. and Easterling, D.R. (2001) The Effects of Climate Change on Stream Flow and Nutrient Loading. *Journal of the American Water Resources Association*, 37(4), 973-985.

Chang, H. (2004) Water Quality Impacts of Climate and Land Use Changes in Southeastern Pennsylvania. *The Professional Geographer*, 56(2), 240-257.

Chang, H. and Jung, I-W. (2010) Spatial and Temporal Changes in Runoff Caused by Climate Change in a Complex Large River Basin in Oregon. *Journal of Hydrology*, 388(3-4), 186-207.

Chang, H. and Lawler, K. (2011) Impacts of Climate Variability and Change on Water Temperature in an Urbanizing Oregon Basin. In *Water Quality: Current Trends and Expected Climate Change Impacts*, IAHS Publication, 348, 123-128.

Chen, H. and Chang, H. (2014) Response of Discharge, TSS, and E. coli to Rainfall Events in Urban, Suburban, and Rural Watersheds. *Environmental Science: Processes and Impacts*, DOI: 10.1039/C4EM00327F

Chiang, L., Yuan, Y., Mehaffey, M. Jackson, M. and Chaubey, I. (2012) Assessing SWAT's Performance in the Kaskaskia River Watershed as Influenced by the Number of Calibration Stations Used. *Hydrological Processes*, DOI: 10.1002/hyp.9589

Choi, W. (2008) Catchment-scale Hydrological Response to Climate-land-use Combined Scenarios: A Case Study for the Kishwaukee River Basins, Illinois. *Physical Geography*, 29(1), 79-99.

City of McMinville [Data] (2011) http://www.ci.mcminnville.or.us/

Cochran, B. and Logue, C. (2011) A Watershed Approach to Improve Water Quality: A Case Study of Clean Water Services' Tualatin River Program. *Journal of the American Water Resources Association*, 47(1), 29–38

CWS (Clean Water Services) [Data] (2011) 16060 SW 85th Ave, Tigard, OR 97224.

Ferrari, R.L. (2001) Henry Hagg Lake 2001 Survey. Sedimentation and River Hydraulics Group. Denver, Co.

Franczyk, J. and Chang, H. (2009) The Effect of Climate Change and Urbanization on the Runoff of the Rock Creek Basin in the Portland Metropolitan Area, Oregon, USA. *Hydrological Processes,* 23, 805-815.

Hanson, G.J. (1990) Surface Erodibility of Earthen Channels at High Stresses. Part II-Developing an In Situ Testing Device. *Transactions of ASAE,* 33, 132-137.

Hatt B.E., Fletcher, T.D. and Deletic, A. (2009) Hydrologic and Pollutant Removal Performance of Stormwater Biofiltration Systems at the Field Scale. *Journal of Hydrology,* 365, 310-321.

Hoyer, M. and Chang. H. (2014a) Development of Future Land Cover Change Scenarios in the Metropolitan Fringe, Oregon, U.S.A. with Stakeholder Involvement. *Land,* 3(1) 322-341.

Hoyer, W. and Chang, H. (2014b) Assessment of Freshwater Ecosystem Services in the Tualatin and Yamhill Basins under Climate Change and Urbanization, *Applied Geography*, 53, 402-416. DOI: 10.1016/j.apgeog.2014.06.023

Kaufmann, P.R., Faustini, J.M., Larsen, D.P. and Shirazi, M.A. (2008) A Roughness-corrected Index of Relative Bed Stability for Regional Stream Surveys. *Geomorphology*, 99, 150-170.

MACA (Multivariate Adaptive Constructed Analogs) Statistical Downscaling Method [Data] (2013) Data Retrieved from: http://nimbus.cos.uidaho.edu/MACA/

Meyer, J.L., Paul, M.J. and Taulbee, W.K. (2005) Stream Ecosystem Function in Urbanizing Landscapes. *Journal of the North American Benthological Society*, 24(3), 602-612.

Moberg, D. (1995) Tualatin Basin Farm Effects on Runoff Quality. Part III: EPIC Model Predictions. USDA – Natural Resources Conservation Service.

Moriasi, D.N, Arnold, J.G., Van Liew, M.W., Bingner, R.L., Harmel, R.D. and Veith, T.L. (2007) Model Evaluation Guidelines for Systematic Quantification of Accuracy in Watershed Simulations. *Transactions of the ASABE*, 50(3), 885-900.

Munoz-Carpena R. and Parsons, J.E. (1999) Modeling Hydrology and Sediment Transport in Vegetative Filter Strips. *Journal of Hydrology*, 214,111-129.

Neitsch, S.L., Arnold, J.G., Kiniry, J.R. and Williams, J.R. (2011) Soil and Water Assessment Tool Theoretical Documentation Version 2009. Texas Water Resources Institute Technical Report No. 406.

NHD (National Hydrography Dataset) Plus (Version 1) [Data] (2010) Retrieved from http://www.horizon-systems.com/nhdplus/

Niraula R., Kalin, L., Srivastava, P. and Anderson, C.J. (2013) Identifying Critical Source Areas of Nonpoint Source Pollution with SWAT and GWLF. *Ecological Modelling,* 268, 123-133.

Oregon Department of Environmental Quality (ODEQ) [Data] (2012) Provided by Eugene Foster from LASAR Database: deq12.deq.state.or.us/lasar2/

Oregon Department of Environmental Quality (ODEQ) (2001) Tualatin Sub-basin Total maximum Daily Load (TMDL): http://www.deq.state.or.us/wq/tmdls/docs/willamettebasin/tualatin/tmdlwqmp.pdf. Last accessed 3/1/2013.

Paul, M.J. and Meyer, J.L. (2001) Streams in the Urban Landscape. *Annual Review of Ecology, Evolution, and Systematics*, 32, 333-365.

Praskievicz, S. and Chang, H. (2009) A Review of Hydrologic Modelling of Basin-Scale Climate Change and Urban Development Impacts. *Progress in Physical Geography*, 33(5), 650-671.

Praskievicz, S. and Chang, H. (2011) Impacts of Climate Change and Urban Development on Water Resources in the Tualatin River Basin, Oregon. *Annals of the Association of American Geographers*, 101(2), 249-271.

Pratt, B. and Chang, H. (2012) Effects of Land Cover, Topography, and Built Structure on Seasonal Water Quality at Multiple Scales. *Journal of Hazardous Materials*, 209/210, 48-58.

Randall, G.W. and Mulla, D.J. (2001) Nitrate Nitrogen in Surface Waters as Influenced by Climatic Conditions and Agricultural Practices. *Journal of Environmental Quality*, 30, 337-344.

Read, J., Wevill, T., Fletcher, T. and Deletic, A. (2008) Variation among Plant Species in Pollutant Removal from Stormwater in Biofiltration Systems. *Water Research*, 42, 893-902.

Runkel, R.L., Crawford, C.G. and Cohn, T.A. (2004) Soad Estimator (LOADEST): A FORTRAN Program for Estimating Constituent Loads in Streams and Rivers. In *Techniques and Methods Book 4*. USGS. Reston, VA.

Singh, S. and Chang, H. (2014) Effects of Land Cover Change on Water Quality in Urban Streams at Two Spatial Scales. *International Journal of Geospatial and Environmental Research*, 1(1), Article 8, Available at: http://dc.uwm.edu/ijger/vol1/iss1/8

Soil Conservation Service (1972) Section 4: Hydrology In *National Engineering Handbook*. SCS.

STATSGO (State Soil Geographic) Database [Data] (2010) Included in SWAT model download: http://swat.tamu.edu/

Sullivan, A.B. and Rounds. S.A. (2005) Modeling Hydrodynamics, Temperature, and Water Quality in Henry Hagg Lake, Oregon, 2000-03. U.S. Geological Survey Scientific Investigations Report 2004-5261 38 p.

Tang, Z., Engel, B.A., Pijanowski, B.C. and Lim, K.J. (2005) Forcasting Land Use Change and its Environmental Impact at a Watershed Scale. *Journal of Environmental Management*, 76, 35-45.

Tong, S.T.Y. and Chen, W. (2002) Modeling the Relationship between Land Use and Surface Water Quality. *Journal of Environmental Management*, 66, 377-393.

Tu, J. (2009) Combined Impact of Climate and Land Use Changes on Streamflow and Water Quality in Eastern Massachusetts, USA. *Journal of Hydrology*, 379, 268-283.

USEPA (2008) Water: Nonpoint Source Success Stories available at http://water.epa.gov/polwaste/nps/success319/OR.cfm

USGS (US Geological Survey). US Land Cover (2011) Retrieved from The USGS Land Cover Institute's website: http://landcover.usgs.gov/uslandcover.php.

USGS (US Geological Survey). National Water Information System (NWIS) (2012) http://waterdata.usgs.gov/nwis/

Vorosmarty, C.J., Green, P., Salisbury, J. and Lammers, R.B. (2000) Global Water Resources: Vulnerability from Climate Change and Population Growth. *Science* 289:284-288.

Wagner, M.M. (2008) Acceptance by Knowing? The Social Context of Urban Riparian Buffers as a Stormwater Best Management Practice. *Society & Natural Resources: An International Journal*, 21(10), 908-920.

Walch, C.J., Roy, A.H., Feminella, J.W., Cottingham, P.D., Groffman, P.M., and Morgan II, R.P. (2005) The Urban Stream Syndrome: Current Knowledge and the Search for a Cure. *Journal of the North American Benthological Society*, 24(3), 706-723.

Whitehead, P.G., Wilby, R.L., Battarbee, R.W., Kernan, M., and Wade, A.J. (2009) A Review of the Potential Impacts of Climate Change on Surface Water Quality. *Hydrological Sciences Journal,* 54(1), 101-123.

Williams, J.R. (1975) Sediment-Yield Prediction with Universal Equation Using Runoff Energy Factor. P. 244-252. In Present and prospective technology for predicting sediment yield and sources: Proceedings of the sediment-yield workshop, USDA Sedimentation Lab., Oxford, MS, November 28-30, 1972. ARS-S-40.

Wilson, D.C., Burns, S.F., Jarrell, W., Lester, Alan, and Larson, E. (1999) Natural Ground-Water Discharge of Orthophosphate in the Tualatin Basin, Northwest Oregon. *Environmental & Engineering Geoscience,* 5(2), 189-197.